J|A|C|S
ARTICLES
Published on Web 01/25/2002

# Phosphonate Lipid Tubules II

Britt N. Thomas,*,† Christopher M. Lindemann,‡ Robert C. Corcoran,§ Casey L. Cotant,§ Janet E. Kirsch,§ and Phillip J. Persichini||

*Contribution from the Department of Chemistry, Louisiana State University, Baton Rouge, Louisiana 70803, Merck & Company, P.O. Box 2000, Rahway, New Jersey 07065, Department of Chemistry, The University of Wyoming, Laramie, Wyoming 82071, and Department of Chemistry, Allegheny College, Meadville, Pennsylvania 16335*

Received September 4, 2001

***Abstract:*** We describe a new chiral tubule-forming lipid in which the C−O−P phosphoryl linkage of the archetypal tubule-forming molecule, 1,2-bis(10,12-tricosadiynoyl)-*sn*-glycero-3-phosphocholine, "DC(8,9)PC", is replaced by a C−P linkage. Tubule formation with this phosphonate analogue proceeds under the same mild conditions as with DC(8,9)PC and produces similar yields, but synchrotron small-angle X-ray scattering, atomic force microscopy, and optical microscopy show the new tubules to have diameters 1.94 times as great, to be significantly shorter, and to be thinner-walled. A significant portion of the enantiomerically pure chiral phosphonate precipitate is in the form of stable open helices, and these helices are divided almost evenly between left- and right-handed members.

## I. Introduction

Dimyristoylphosphatidylcholine and dipalmitoylphosphatidylcholine analogues in which diacetylene groups have been inserted midway in the long hydrocarbon tails self-assemble to yield tubules − stable, hollow cylindrical crystalline vesicles, as first reported by Yager and co-workers[1−4] in 1984. The *S*-enantiomer of the prototypical tubule-forming molecule, 1,2-bis(10,12-tricosadiynoyl)-*sn*-glycero-3-phosphocholine, **1**, hereafter referred to as "DC(8,9)PC", is shown in Figure 1.

Tubules made from DC(8,9)PC and analogues in which the diacetylene moiety is repositioned along the hydrocarbon tails display a single helical trace upon their exteriors, suggesting these cylindrical structures are the product of the helical winding of a phospholipid bilayer ribbon. A remarkable correspondence between the sense of handedness of this helical trace and DC(8,9)PC monomer chirality is known: the *R*-DC(8,9)PC monomer always produces tubules that have a right-handed exterior helical trace, while the *S*- enantiomer always yields tubules that have a left-handed exterior helical trace. This widely known correspondence has served as the impetus for a number of tubule structure theories that link helix handedness to molecular chirality.[5−12] Another intriguing aspect of tubule structure is seen in tubules formed in ethanolic solvents; these tubules are multilamellar, that is, they are made of several evenly

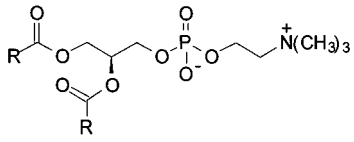


**1**

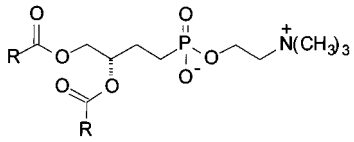


**2**

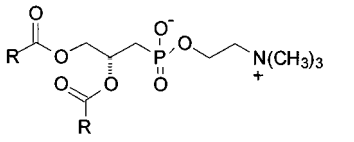


**3**

***Figure 1.*** (top) DC(8,9)PC. (middle) Compound **2**, the "C4" phosphonate analogue of DC(8,9)PC. (bottom) Compound **3**, the "C3" phosphonate analogue of DC(8,9)PC.

* To whom correspondence should be addressed.
† Louisiana State University.
‡ Merck & Co.
§ The University of Wyoming.
|| Allegheny College.

(1) Schoen, P. E.; Yager, P.; Priest, R. G. *NATO Sci. Ser., Ser. E* **1985**, *102-(Polydiacetylenes)*, 223−232.
(2) Yager, P.; Schoen, P. E.; Davies, C.; Price, R.; Singh, A. *Biophys. J.* **1985**, *48*, 899−906.
(3) Schoen, P. E.; Yager, P. *J. Polym. Sci., Polym. Phys. Ed.* **1985**, *23*, 2203−2216.
(4) Yager, P.; Schoen, P. E. *Mol. Cryst. Liq. Cryst.* **1984**, *106*, 371−381.
(5) de Gennes, P. G. *C. R. Acad. Sci. Paris* **1987**, *304*, 259.
(6) Helfrich, W.; Prost, J. *Phys. Rev. A: Gen. Phys.* **1988**, *38*, 3065−3068.
(7) Helfrich, W. *J. Chem. Phys.* **1986**, *85*, 1085−1087.
(8) Lubensky, T. C.; Prost, J. *J. Phys. II* **1992**, *2*, 371−382.
(9) Ou-Yang, Z.; Liu, J. *Phys. Rev. Lett.* **1990**, *65*, 1679−1682.
(10) Selinger, J. V.; Schnur, J. M. *Phys. Rev. Lett.* **1993**, *71*, 4091−4094.
(11) Selinger, J. V.; MacKintosh, F. C.; Schnur, J. M. *Phys. Rev. E: Stat. Phys., Plasmas, Fluids, Relat. Interdiscip. Top.* **1996**, *53*, 3804−3818.
(12) Schnur, J. M. *Science* **1993**, *262*, 1669−1676.

spaced coaxially nested cylinders. Interestingly, it has recently been demonstrated that the tubule interior lamellae may have either a left- or a right-handed helical sub-structure.[13]

Tubule dimensions and morphology, particularly their hollowness, have suggested a host of potential technological applications, ranging from nanofabrication and purification to medical encapsulation.[12,14−16] Realization of the full technological potential of tubules requires the ability to optimize their morphology for a given application. While tubule length is moderately controllable over a range of a few microns to hundreds of microns through solvent composition[17] or kinetics control,[18] tubule diameter has proven to be insensitive to regulation.

In previous work,[19] we reported a 2-fold increase in tubule diameter attained through a subtle modification to DC(8,9)PC, the replacement of the phosphoryl oxygen linking the glycerol backbone to the phosphocholine headgroup with a methylene ($-CH_2-$) group, resulting in DC(8,9)PC phosphonate analogue **2**. Our synthesis of **2** was motivated by the predicted dependency of tubule diameter upon chiral packing of the tubule-forming molecules within the lamellae.[10−12] We speculated that small changes in bond lengths and angles near the stereogenic center might be sufficiently subtle to conserve tubule-forming capacity, yet large enough by virtue of their placement to affect product morphology.

Concurrent with the 2-fold diameter increase found with tubules derived from **2** was a halving of the tubule wall thickness. That is, the number of coaxially nested cylinders composing the phosphonate tubule wall was found to be half that found for DC(8,9)PC tubules. Despite the large changes to tubule diameter and wall thickness, the space between the coaxial cylindrical lamellae was virtually unchanged. Tubule length was also unaffected. Comparatively large numbers of open helices were found in the DC(8,9)PC phosphonate analogue preparations, that is, helically wound ribbons whose widths are too narrow to enable fusion of the ribbon edges to form closed cylinders. Very surprisingly, the open helices and the fully formed tubules in this system were found to violate the widely known helical handedness/molecular chirality correspondence; indeed, roughly equal numbers of left-handed and right-handed helices and tubules were formed from enantiomerically pure preparations. Helical structures of the unexpected sense of handedness have subsequently been described in the study of an enantiomerically pure, multicomponent (water, bile salt, phosphatidylcholine, and cholesterol) system,[20] although one sense of handedness is found to be dominant in this model bile system.

The success obtained by substituting the DC(8,9)PC linking phosphoryl oxygen with a ($-CH_2-$) group has motivated the synthesis and study of DC(8,9)PC phosphonate analogue **3**, in which the polar headgroup has been moved closer to the stereogenic center contained within the glycerol backbone. This translation is accomplished through the *removal* of the linking phosphate oxygen atom, rather than the ($-CH_2-$) replacement that led to phosphonate analogue **2**. The ($-CH_2-$)-for-oxygen substitution leading to phosphonate analogue **2** resulted in the lengthening of the DC(8,9)PC three-carbon glycerol backbone to four contiguous carbon atoms, which led us to conveniently refer to **2** as the "C4" phosphonate; in the same manner we refer to the molecule of this study, phosphonate analogue **3**, as the "C3" phosphonate.

## II. Experimental Section

**II.a. Synthesis. II.a.1. General Procedures.** Methylene chloride and pyridine were distilled from $CaH_2$ and solid KOH, respectively. Triethyl phosphite was distilled under reduced pressure prior to use. 1,2:5,6-Di-*O*-isopropylidene-D-mannitol, bromotrimethylsilane, 4-(dimethylamino)pyridine, carbon tetrabromide, and choline chloride were purchased from Aldrich. 10,12-Tricosadiynoic acid was purchased from Lancaster. All of these materials were used without any further purification. Silica gel 60 (230−400 mesh) was used for column chromatography. $^1$H and $^{13}$C NMR spectra were obtained in $CDCl_3$ solutions at 270 and 67.5 MHz, respectively. The high-resolution mass spectrum of compound **3** was obtained by the Washington University Resource for Biomedical and Bio-organic Mass Spectrometry at Washington University, St. Louis, Missouri.

**II.a.2. (*S*)-4-Hydroxymethyl-2,2-dimethyl-1,3-dioxolane (4).** A solution of 1,2:5,6-di-*O*-isopropylidene-D-mannitol (10.5 g, 40 mmol) in ethyl acetate (160 mL) was cooled to 0 °C (during which time the mannitol crystallized). The ice bath was removed, and lead tetraacetate (17.8 g, 40.2 mmol) was added in portions over a 10 min time period. After an additional 35 min the reaction was filtered. The precipitate was washed with ethyl acetate, and the combined organics were washed with brine/saturated sodium bicarbonate (1:1, 2 × 20 mL) and brine (20 mL) and were dried ($Na_2SO_4$). To this solution was added ethanol (20 mL) followed by portionwise addition of sodium borohydride (5.2 g). After the last addition, acetone (10 mL) was added, and the solution was diluted with diethyl ether (250 mL) and carefully washed with 1:1 brine/5% aqueous HCl (2 × 50 mL), brine (50%, 50 mL), and brine/saturated bicarbonate (50 mL) and was dried ($Na_2SO_4$) and concentrated under reduced pressure. The residue was brought up in methanol (175 mL) which had been saturated with ammonia gas, left to stand 12 h, and again concentrated under reduced pressure. The crude material was purified by flash chromatography on silica gel using a gradient elution from hexane/ethyl acetate (3:1) to ethyl acetate (100%) to give (*S*)-4-hydroxymethyl-2,2-dimethyl-1,3-dioxolane, **4** (4.56 g, 86.4%), having $^1$H and $^{13}$C NMR identical to published spectral data.[21]

**II.a.3. (*R*)-4-Bromomethyl-2,2-dimethyl-1,3-dioxolane (5).** A solution of triphenylphosphine (8.33 g, 31.8 mmol) in $CH_2Cl_2$ (15 mL) was added dropwise over a 9 h period (via syringe pump) to a well-stirred solution of **4** (4.22 g, 31.9 mmol) and carbon tetrabromide (13.98 g, 42.2 mmol) in $CH_2Cl_2$ (8 mL) at room temperature. The reaction was diluted with hexane (200 mL) and washed with aqueous sodium bicarbonate (5%, 40 mL) and brine (40 mL) and was dried ($Na_2SO_4$) and concentrated. The crude material was purified by flash chromatography on silica gel using hexane/ethyl acetate (5:1) to give (*R*)-4-bromomethyl-2,2-dimethyl-1,3-dioxolane, **5** (2.15 g, 34.5%). $^1$H NMR: $\delta$ 4.35 (m, 1H), 4.12 (dd, 1H, $J$ = 12 Hz, 9 Hz), 3.87 (dd, 1H, $J$ = 9 Hz, 6 Hz), 3.45 (dd, 1H, $J$ = 9 Hz, 6 Hz), 3.33 (dd, 1H, $J$ = 12 Hz, 9 Hz), 1.45 (s, 3H), 1.35 (s, 3H).

**II.a.4. Diethyl [(*R*)-*O*-3,4-Isopropylidene-3,4-dihydroxypropyl] Phosphonate (6).** A solution of **5** (2.05 g, 10.5 mmol) in triethyl

(13) Thomas, B. N.; Lindemann, C. M.; Clark, N. A. *Phys. Rev. E* **1999**, *59*, 3040−3047.
(14) Archibald, D. D.; Mann, S. *Chem. Phys. Lipids* **1994**, *69*, 51−64.
(15) Baum, R. *Chem. Eng. News* **1993**, *August 9*, 19−20.
(16) Johnson, D. L.; Polikandritou-Lambros, M.; Martonen, T. B. *Drug Delivery* **1996**, *3*, 9−15.
(17) Ratna, B. R.; Baral-Tosh, S.; Kahn, B.; Schnur, J. M.; Rudolph, A. S. *Chem. Phys. Lipids* **1992**, *63*, 47−53.
(18) Thomas, B. N.; Safinya, C. R.; Plano, R. J.; Clark, N. A. *Science* **1995**, *267*, 1635−1638.
(19) Thomas, B. N.; Corcoran, R. C.; Cotant, C. L.; Lindemann, C. M.; Kirsch, J. E.; Persichini, P. J. *J. Am. Chem. Soc.* **1998**, *120*, 12178−12186.
(20) Zastavker, Y. V.; Asherie, N.; Lomakin, A.; Pande, J.; Donovan, J. M.; Schnur, J. M.; Benedek, G. B. *Proc. Natl. Acad. Sci. U.S.A.* **1999**, *96*, 7883−7887.
(21) Pouchert, C. J.; Behnke, J. *The Aldrich Library of $^{13}$C and $^1$H FT-NMR Spectra*; Aldrich Chemical Co.: Milwaukee, Wisconsin, 1983.

***Scheme 1.*** Synthesis of DC(8,9)PC Phosphonate Analog **3**[a]

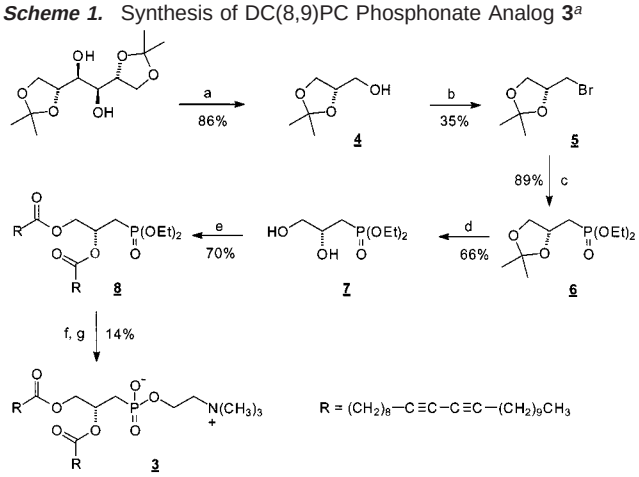


[a] (a) $Pb(OAc)_4$, $NaBH_4$; (b) $P(Ph)_3$, $CBr_4$; (c) $P(OEt)_3$, Δ; (d) *p*-TsOH, EtOH; (e) 10,12-tricosadiynoic acid, DMAP, DCC, $CH_2Cl_2$; (f) $(CH_3)_3SiBr$, $CH_2Cl_2$, THF, $H_2O$; (g) choline chloride, $Cl_3CCN$, pyridine.

phosphite (12 mL, 70.0 mmol) was refluxed for 14 h. The residual triethyl phosphite was removed under reduced pressure, and the crude product was purified by flash chromatography on silica gel using ethyl acetate to give diethyl [(*R*)-*O*-3,4-isopropylidene-3,4-dihydroxypropyl] phosphonate **6** (2.37 g, 89.4%). $^1$H NMR: $\delta$ 4.38 (m, 1H), 4.13 (m, 5H), 3.68 (dd, 1H, $J$ = 11 Hz, 7.5 Hz), 2.33−1.91 (m, 2H), 1.43−1.11 (m, 12H).

**II.a.5. Diethyl [(*R*)-3,4-Dihydroxypropyl] Phosphonate (7).** A solution of **6** (1.91 g, 7.6 mmol) and *p*-toluenesulfonic acid (211 mg, 1.1 mmol) in ethanol (70 mL) was stirred for 14 h at room temperature under a $N_2$ atmosphere. The mixture was neutralized with solid sodium bicarbonate, filtered, and concentrated under reduced pressure. The residue was brought up in $CHCl_3$ (50 mL) and filtered through Celite. This material was concentrated under reduced pressure and purified by flash chromatography on silica gel using $CHCl_3$/$CH_3OH$ (7:1) to give diethyl [(*R*)-3,4-dihydroxypropyl] phosphonate **7** (1.06 g, 66.3%). $^1$H NMR: $\delta$ 4.12 (m, 5H), 3.70 (m, 1H), 3.54 (dd, 1H, $J$ = 12 Hz, 6 Hz), 2.42 (bs, 2H), 2.12−1.87 (m, 2H), 1.35 (dt, 6H, $J$ = 7.5 Hz, 3 Hz).

**II.a.6. Diethyl [(*S*)-3,4-Bis(10,12-tricosadiynoyloxy)propyl] Phosphonate (8).** A solution of 1,3-dicyclohexylcarbodiimide (2.27 g, 11.0 mmol) in dry $CH_2Cl_2$ (7 mL) was added to a stirred solution of diethyl phosphonate **7** (1.06 g, 5.0 mmol), 10,12-tricosadiynoic acid (3.64 g, 10.5 mmol), and (dimethylamino)pyridine (128.3 mg, 1.05 mmol) in dry $CH_2Cl_2$ (35 mL) and was stirred under a $N_2$ atmosphere. After stirring for 48 h at room temperature, the reaction mixture was filtered through Celite, and the filtrate was evaporated to furnish a light-yellow solid. The solid was purified by flash chromatography on silica gel using hexane/ethyl acetate (2:1) to give diethyl [(*R*)-3,4-bis(10,12)-tricosadiynoyloxy)propyl] phosphonate **8** (3.06 g, 70.4%). $^1$H NMR: $\delta$ 5.36 (m, 1H), 4.40 (dd, 1H, $J$ = 12 Hz, 3 Hz), 4.12 (m, 5H), 2.37−2.11 (m, 14H), 1.70−1.20 (m, 62H), 0.93 (t, 6H, $J$ = 7.5 Hz).

**II.a.7. 1-[(*S*)-3,4-Bis(10,12-tricosadiynoyloxy)propyl] Phosphonic Acid, 2-(*N*,*N*,*N*-Trimethylammonium) Ethyl Ester (3).** Bromotrimethylsilane (1.21 mL, 9.91 mmol) was added over a period of 1 h to a stirred solution of diethyl [(*S*)-3,4-bis(10,12-tricosadiynoyloxy)propyl] phosphonate **8** (3.06 g, 3.52 mmol) in dry $CH_2Cl_2$ (7 mL) under a $N_2$ atmosphere. Six hours after completion of the addition, the reaction mixture was concentrated in vacuo, the residue was brought up in aqueous THF (10%, 15 mL), and the solution was heated at reflux for 90 min. The solvent was removed under reduced pressure, and the residue was dissolved in $CHCl_3$ (30 mL). The $CHCl_3$ solution was dried ($Na_2SO_4$), filtered, and concentrated under reduced pressure to give 2.80 g (98%) of phosphonic acid which was utilized without any further purification (Scheme 1).

A suspension of the phosphonic acid, choline chloride (2.27 g, 16.3 mmol), and dry pyridine (125 mL) was heated to 60 °C under a $N_2$ atmosphere. Trichloroacetonitrile (15.23 mL) was added, and the reaction was stirred at 60 °C for 44 h. The solvent was removed under reduced pressure, and the residue was dissolved in $CH_2Cl_2$. Activated carbon was added to the solution, and the mixture was filtered through Celite. The filtrate was concentrated under reduced pressure, and the crude product was purified by flash chromatography on silica gel using $CHCl_3$/$CH_3OH$/$H_2O$ (2:0.8:0.15) to give 1-[(*S*)-3,4-bis(10,12-tricosadiynoyloxy)propyl] phosphonic acid, 2-(*N*,*N*,*N*-trimethylammonium) ethyl ester **7** (580 mg). This material was further purified by trituration with acetone to afford 347.8 mg (14.0%). $^1$H NMR: $\delta$ 5.24 (m, 1H), 4.57 (m, 1H), 4.34 (m, 2H), 4.07 (m, 1H), 3.81 (m, 2H), 3.35 (bs, 9H), 2.24 (m, 12H), 1.90 (m, 2H), 1.26−1.55 (m, 56H), 0.88 (t, 6H, $J$ = 6.5 Hz). $^{13}$C NMR (67.5 MHz): $\delta$ 173.3, 173.2, 77.60, 77.58, 77.39, 76.93, 71.80 (d, $J$cp = 15.3 Hz), 66.86, 65.28, 65.19, 64.85, 57.66, 54.54, 34.43 (d, $J$cp = 31.4 Hz), 31.86, 30.89, 29.61, 29.59, 29.57, 29.54, 29.51, 29.48, 29.45, 29.43, 29.41, 29.39, 29.28, 29.12, 29.07, 28.93, 28.84, 28.80, 28.33, 25.60, 24.87 (d, $J$cp = 17.3 Hz), 22.65, 19.17, 14.10. $^{31}$P NMR (132 MHz, 85% $H_3PO_4$ external reference): $\delta$ 18.59. HRMS calcd for $C_{54}H_{93}NO_7P$: 898.6689. Found: 898.6685.

**II.b. Physical Characterization. II.b.1. Tubule Preparation.** DC(8,9)PC and "C3" phosphonate tubules were prepared by adding 1 mg of lipid to 1 mL of EtOH/$H_2O$ solvent, heating to 50 °C with vigorous stirring, and cooling the clear solutions to room temperature to obtain flocculent off-white precipitates. Solvent compositions that maximized precipitate yields for DC(8,9)PC and the "C3" phosphonate **3** were 0.7:0.3 and 0.6:0.4 (v:v), respectively; these solvent compositions were used throughout the work presented in this report. It has been shown that DC(8,9)PC tubule lengths depend not only upon the solvent composition,[17] but upon the rate at which the spherical vesicles from which they form are cooled[18] as well. Accordingly, the DC(8,9)PC and the "C3" phosphonate preparations were driven through their tubule formation temperatures (38 and 37 °C for DC(8,9)PC and the "C3" phosphonate, respectively) at the same rate, 12.8 °C/h. Tubule yields were determined by centrifuging and desiccating the precipitate to constant mass.

**II.b.2. Optical Microscopy.** Differential interference contrast microscopy (DIC) was conducted with a Nikon Diaphot 300 inverted microscope equipped with 60× and 100× Nomarski objectives, and images were digitized using a Dage VE1000 CCD video camera coupled to a high-resolution video capture board or were photographed with a Nikon N6006 35 mm camera. Tubule lengths were tabulated on a Macintosh computer using the public domain NIH Image program, developed at the U.S. National Institutes of Health, and are available on the Internet at http://rsb.info.nih.gov/nih-image/. All specimens were handled as gently as possible to minimize tubule breakage.

**II.b.3. Atomic Force Microscopy.** Contact- and tapping-mode atomic force microscopy probes were conducted on a vibrationally and thermally isolated Digital Instruments BioScope, equipped with silicon nitride NanoProbe SPM tips. Tubule external diameters were measured by determining the perimeter of the cross-sectional AFM trace of the tubule and dividing by $\pi$. Finite tip-size convolution error has been found to be negligible.[19] Local membrane elasticity probes were conducted on a Digital Instruments Nanoscope IIIa Multi-Mode scanning probe microscope using oxide-sharpened silicon nitride tips.[19]

**II.b.4. X-ray Diffraction.** High-resolution small-angle X-ray scattering was done at Beamline X20A of the National Synchrotron Light Source at Brookhaven National Laboratory. X-rays (1.6122 Å) were used with an in-plane resolution of 0.0007 Å$^{-1}$, commensurate with the Ge[1,1,1] analyzer crystal, while out-of-plane resolution was relaxed to 0.008 Å$^{-1}$ to increase signal intensity. Tubule samples of $c \approx 100$ mg lipid/mL were prepared by centrifuging at 10 000*g* at 20 °C for 30 min; optical microscopy of the resuspended pellet revealed no discernible change in tubule morphology induced by centrifugation. This

concentrated paste was placed in standard 1.5 mm diameter quartz diffraction capillaries, yielding unoriented (powder) samples.

Tubules polymerize upon exposure to ionizing radiation and acquire a deep purple color in time intervals well below those required for X-ray data acquisition. Radiation damage was minimized by translating 50 mm of the 80 mm capillary length continuously through the ~0.5 mm tall collimated X-ray beam during data acquisition, which had the effect of dispersing radiation damage throughout an approximately 100-fold larger powder sample than a stationary sample would present. Accordingly, one should expect a diminution of radiation damage as great as 2 orders of magnitude.[22] Complete data sets were acquired with markedly less sample discoloration and presumably less radiation-induced damage. Each point in reciprocal space was acquired with an integral number of sample translations to ensure that any chance sample inhomogeneities and domain alignments were distributed evenly throughout the reciprocal space scan.

The instrument resolution was deconvolved from the tubule interlamellar (00*l*) peak and fit to the powder average of the scattering from infinite length multilayer tubule structures having outer diameter *D*, wall thickness *T*, and layer spacing *d*. DC(8,9)PC and "C4" phosphonate tubules formed in ethanol/water solvent systems are known to be composed of coaxially nested hollow cylindrical lamellae, and this is also the case with tubules formed from the "C3" phosphonate **2**. These nested layers were assumed to be perfect cylinders, corresponding to membranes with no bending fluctuations, that is, rigid membranes.[23,24] From this model and the measured half-width at half-maximum, we obtained a correlation length $\xi$ which we take to be the mean tubule wall thickness. Because both phosphonate and DC(8,9)PC tubule outer diameters *D* are rather narrowly distributed, determination of the correlation length $\xi$ and the lamellar spacing *d* permits estimation of the number of lamellae comprising the tubule wall.

## III. Results

**III.a. Tubule Yields.** The straightforward measure of how well tubule-forming capacity has been conserved is to compare DC(8,9)PC and "C3" phosphonate tubule yields. This proved difficult, however, for small amounts of irregular granules, approximately 1 $\mu$m in diameter, were present in the "C3" phosphonate preparations. These granules are absent in the corresponding dilute DC(8,9)PC and "C4" phosphonate preparations, but are identical in appearance to the bulk lamellar coprecipitate that forms in overly concentrated DC(8,9)PC solutions. We were unable to separate the two morphologies. In view of the apparent similarity to granules formed in overly concentrated DC(8,9)PC solutions, we decreased the "C3" phosphonate concentrations used for tubule formation, but the granules continued to appear even when the lipid concentration was reduced 20-fold. The possibility that the granules are merely undissolved bulk lipid was investigated by vigorously stirring dilute phosphonate solutions at 75 °C for extended periods prior to tubule formation, but the same results were obtained. On the basis of extensive microscopic observations indicating that a very small percentage of the microscope field-of-view is occupied by these granules, and taking into account that tubules are hollow and the granules appear solid, we can estimate roughly that less than 5% of the "C3" phosphonate precipitate by mass is in the form of granules. The *overall* "C3" phosphonate precipitate yield (comprising tubules and granules) is 90%, the value found for DC(8,9)PC and "C4" phosphonate tubule yields. Deduction of the small percentage of granular precipitate from the overall "C3" phosphonate yield leads us to conclude that tubule-forming capacity has not been substantially altered as a result of the changes made to the DC(8,9)PC backbone.

**III.b. Tubule Gross Morphology.** The most striking morphological difference between tubules made from the "C3" phosphonate analogue **3** and DC(8,9)PC is a 1.94-fold increase in external diameter. Contact-mode atomic force microscopy yielded a mean "C3" phosphonate tubule external diameter of $1.076 \pm 0.090$ $\mu$m; the same protocol yielded a mean diameter determination of $0.554 \pm 0.053$ $\mu$m for DC(8,9)PC tubules. Tubules made from the previously studied "C4" phosphonate **2** were found to have a mean diameter of $1.182 \pm 0.135$ $\mu$m. Because the AFM probe used to determine these micron-scale tubule diameters has nanometer-scale resolution, the uncertainties we report are essentially the standard deviations of the respective distributions about the mean values. It is evident from the narrow (approximately ±10%) standard deviations that the "C3" and "C4" phosphonate mean tubule diameters, while close, are nevertheless distinct.

Tubule lengths were measured microscopically, and once again comparison of the instrument resolution to the magnitude of measured quantity leads to uncertainties that are essentially standard deviations about the mean. It was found that length deviations for all three systems are large, being about ±50% of the mean value. As a result, the DC(8,9)PC and the previously studied "C4" phosphonate tubule lengths, $25.8 \pm 12.7$ $\mu$m and $23.5 \pm 11.1$ $\mu$m respectively, may be considered to be essentially indistinguishable. In contrast, the $16.6 \pm 8.6$ $\mu$m mean length of the "C3" phosphonate tubules of this study is significantly smaller. Because all three preparations were handled identically and with great care to avoid tubule breakage, we interpret shorter "C3" phosphonate tubule mean length to be an intrinsic property of the "C3" phosphonate self-assembly product.

**III.c. Phosphonate Tubule Membrane Deformability.** Tubules derived from phosphonates **2** and **3** appear to be more flexible than those made of DC(8,9)PC and are often partially unwound at the tubule end, as seen in the Nomarski differential interference contrast micrograph of Figure 2. Phosphonate tubules also deform through flattening upon drying. This deformability was discovered in the course of AFM probes of tubule structure; while tubules sink in solution and lie atop the substrate, they remain mobile and are pushed about by the probing AFM tip, necessitating air-drying to fix them. The extent of the resultant flattening in the "C3" and "C4" phosphonate tubules is so great, however, that the height difference between alternating helix segments was found to be of the same magnitude, or less, than that of the flattened ribbon roughness. The membrane elasticity suggested by this deformation was characterized through local force-modulation AFM. In this technique, the AFM tip is forced down upon the sample, and the amplitude of the cantilever tip deflection versus height above the sample is measured. The magnitude of the oscillating cantilever's deflection as it is pushed onto the sample is inversely related to the extent of indentation induced in the sample. A "soft" sample will deform with little resistance as the AFM tip approaches, causing only a small change in the amplitude of the oscillating AFM cantilever deflection. We found the AFM cantilever tip had to be driven with 1.25× greater amplitude with "C3" phosphonate tubules to obtain the same deflection

(22) Thomas, B.; Safinya, C. R.; Plano, R. J.; Clark, N. A.; Ratna, B. R.; Shashidar, R. *Mater. Res. Soc. Symp. Proc.* **1992**, *248*, 83−88.
(23) Safinya, C. R.; Roux, D.; Smith, G. S.; Sinha, S. K.; Dimon, P.; Clark, N. A.; Nellocq, A. M. *Phys. Rev. Lett.* **1986**, *57*, 2718−2721.
(24) Roux, D.; Safinya, C. R. *J. Phys. (Paris)* **1988**, *49*, 307−0318.

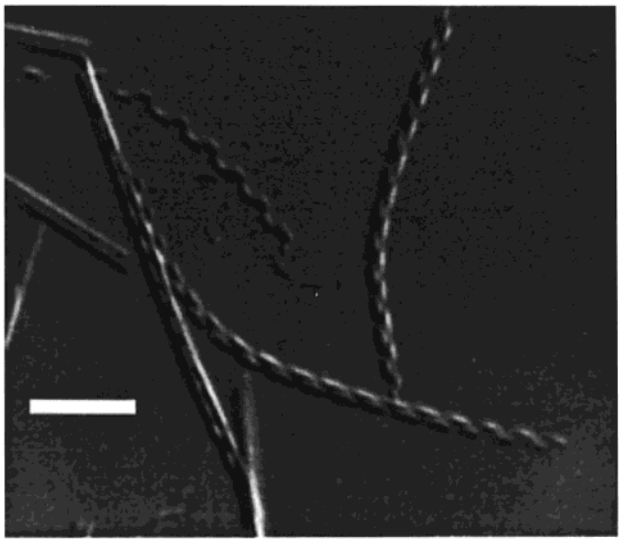

***Figure 2.*** Nomarski differential interference contrast micrograph of "C3" phosphonate tubules. Notice the gentle bending of the tubule axes and the unwinding occurring at the tubule ends. The vertical tubule found at the right of the figure and the diagonal tubule it touches appear to have opposite senses of handedness. The scalebar is 5 $\mu$m long.

obtained with DC(8,9)PC tubules, indicating significantly greater "C3" phosphonate tubule wall elasticity. The identical technique applied to the previously studied "C4" phosphonate tubules indicated an even greater elasticity; the cantilever tip had to be driven with 1.77× greater amplitude over that required for DC(8,9)PC tubules.

**III.d. Tubule and Helix Handedness.** The desiccation-induced flattening unexpectedly reduced the height differences between alternating helix segments to that of membrane surface roughness, frustrating straightforward attempts to determine helix handedness through acquiring AFM height maps. It was found, however, that water immersion of air-dried, fixed specimens caused the tubules and helices to resume their unflattened shape, yet remain fixed to the substrate, enabling underwater contact-mode AFM.[19] It was found that, as is the case with the "C4" phosphonate **2**, open helices formed from the enantiomerically pure "C3" phosphonate **3** had roughly equal probabilities of being right- or left-handed.

Corroborating evidence supporting our "mixed" handedness findings comes from Nomarski Differential Interference Contrast (DIC) microscopy probes of undesiccated phosphonate tubules. In the inverted microscope configuration utilized, the tubules sink to the bottom of the ethanolic solution and lie atop the glass coverslip. The ability to consistently and unambiguously focus upon the side of unflattened helices in contact with the coverslip has been demonstrated,[19] and because optically probed helices need not be fixed and may remain in solvent, flattening does not occur. The intersection of the narrow microscope focal plane with the near side of an open helically wound ribbon yields a two-dimensional alternating pattern of ribbon and interstitial void. As long as the microscope focal plane is unequivocally placed at the helix side nearest the observer, the helical handedness generating this pattern is resolvable in the same way that the sense of handedness of a machine screw may be ascertained from its two-dimensional photograph. We detected left- and right-handed helices in nearly equal numbers, a finding in agreement with the AFM probes and similar to our earlier "C4" phosphonate tubule results.

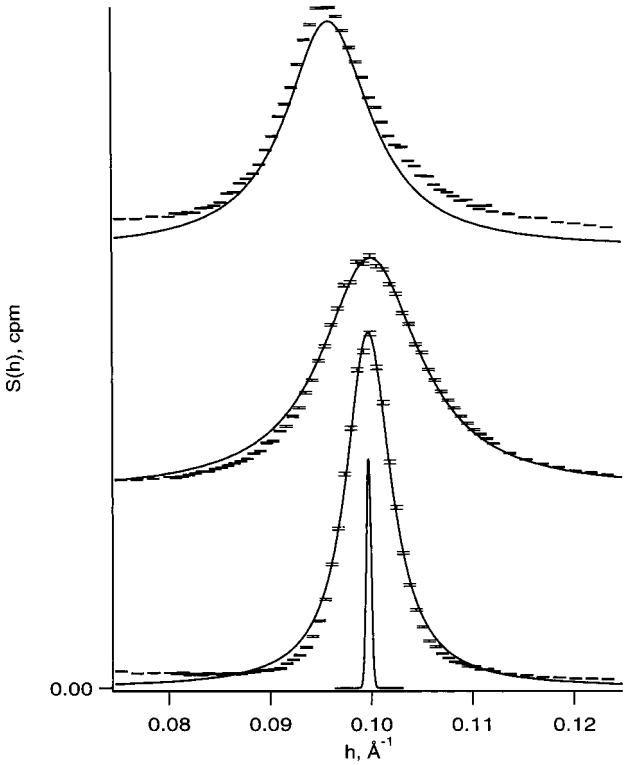


***Figure 3.*** Small-angle X-ray scattering showing the interlamellar fundamental peaks from "C4" phosphonate tubules (top), "C3" phosphonate tubules (middle), and DC(8,9)PC tubules (bottom). The data are drawn to the same scale but offset vertically for clarity. The solid trace is the 0.0007 Å$^{-1}$ fwhm instrument resolution, drawn to a different vertical scale. Differences in peak intensities are attributable to differences in tubule suspension concentrations in the three samples.

It should be noted that while Nomarski DIC is capable of resolving the sense of handedness of an open helix, it is generally incapable of doing so with fully formed tubules. DIC optics are designed to enhance the index of refraction discontinuity found at object-solution interfaces, such as at the ribbon edges, but no such discontinuity exists along the fused helical trace of fully formed, closed tubules. AFM examination of the helical ridges found upon "C3" phosphonate tubules shows them to be far less pronounced than those found upon DC(8,9)PC tubule exteriors. This comparative smoothness, in conjunction with the propensity of phosphonate tubules to flatten, made AFM handedness determination of fully formed phosphonate tubules considerably more difficult than with DC(8,9)PC tubules. Nevertheless, AFM probes reveal roughly equal numbers of right- and left-handed exterior helical traces on fully formed "C3" phosphonate tubules.

**III.e. Phosphonate Tubule Internal Structure.** Small-angle X-ray scattering (SAXS) data from DC(8,9)PC, "C4", and "C3" phosphonate tubule suspensions are given in Figure 3. The DC(8,9)PC, "C4", and "C3" phosphonate tubule (00*l*) peaks are centered at $|k_0| = 4\pi \sin(2\theta/2)/\lambda = 0.0998$, 0.09624, and 0.100346 Å$^{-1}$, respectively. Despite the differences in tubule diameters for the three compounds, the interlamellar spacings *d* are quite close: 62.97 Å for DC(8,9)PC and 65.29 and 62.62 Å for the "C4" and "C3" phosphonates, respectively. It is worth noting that the DC(8,9)PC interlamellar spacing lies *between* that of the two phosphonates. We interpret this remarkable conservation of interlamellar spacing throughout a 2-fold increase in tubule diameter as an indication of the relative

importance of interlamellar forces in comparison to those that determine the cylindrical radii of curvature for the three systems.

Peak-shape analyses for completely rigid membranes leads to a correlation length for the "C3" phosphonate $\xi_{C3} = 197.9$ Å, whereas for DC(8,9)PC and the "C4" phosphonate tubules the correlation lengths were $\xi_{DC(8,9)PC} = 431.08$ Å and $\xi_{C4} = 207.0$ Å, respectively. Because of the narrow dispersion of tubule diameters for each molecule, we interpret these values to be equivalent to the tubule wall thickness *T*. The ratio of tubule wall thickness to interlamellar spacing is the number *n* of bilayers composing the tubule; we find *n* to be 6.9 for DC(8,9)PC and 3.2 for both phosphonates, a finding intuitively consistent with the observed phosphonate tubule flattening and deformability. Thus, we find that the two phosphonates produce tubules having nearly identical wall thicknesses (about half that of tubules made from DC(8,9)PC) and with similarly close cylindrical diameters (about twice that of DC(8,9)PC tubules).

While the number of coaxially nested cylinders composing tubules is the same for both phosphonates, as is the interlamellar distance between these cylinders, the AFM-determined surface normal elasticities are not equal. Because the AFM probe was applied to "C3" and "C4" phosphonate tubules having the same number of lamellae as well as interlamellar separation, we surmise that the elasticity variation reflects a structural difference intrinsic to the lamellae. That is, the elasticity variation is not a consequence of different tubule wall thicknesses offering more or less resistance to the AFM probe tip. We note that the more elastic "C4" phosphonate membrane produces tubules with the largest diameter. If we set aside wall thickness considerations momentarily and extend our comparison to include DC(8,9)PC tubules, we find this trend continues; the least elastic membrane is associated with the smallest diameter tubule. Because our phosphonate study is currently limited to two molecules, and we include DC(8,9)PC in this comparison as well, it is premature to conclude that a membrane elasticity/tubule diameter correlation exists, although it is in accord with the limited amount of data.

## IV. Discussion

The self-assembly behaviors exhibited by phosphonates **2** and **3** raise a number of questions regarding the role of molecular structure, particularly chirality, in determining tubule handedness and dimensions. Specifically, the surprising observation of stable right- and left-handed helices in enantiopure phosphonate preparations suggests helix formation can be statistical in nature, rather than being based in chiral intermolecular interactions. For example, a tilt-driven spontaneous chiral symmetry breaking of the membrane that would produce both senses of helical handedness has been proposed.[25] Within this theory's framework, chiral membranes may result even from achiral molecules, and the random tilt direction chosen by the ensemble should produce our experimentally observed ~50:50 ratio of left- to right-handed helical structures. The helix may be otherwise viewed as a *macroscopic* breaking of chiral symmetry, analogous to the spiral defects seen in freely suspended hexatic films of chiral molecules.[26] No dependence of the spiral's sense of handedness upon molecular chirality is found in these systems, and it has been speculated that localized impurities, rapid formation kinetics, or thermal fluctuations that nucleate vortex−antivortex pairs are the origins of these chiral defects.[27]

At the same time, the striking uniformity of the helical trace found on enantiopure DC(8,9)PC tubule *exteriors* cannot be ignored. If a statistical mechanism in determining helical handedness is operative, molecular chirality must, at least in the case of DC(8,9)PC, overwhelmingly bias the otherwise random ensemble tilt. The corresponding lack of uniformity in the equilibrium phosphonate tubule preparations indicates that, whatever mechanism is in effect, the modifications we have installed near the DC(8,9)PC stereogenic center have substantially diminished the influence that molecular chirality exerts upon self-assembly product morphology.

A key prediction of chiral-packing theories is that tubule diameter is a consequence of chiral intralamellar packing efficiency. In racemic mixtures, one would expect chiral packing effects to average to zero, and the theory predicts tubule diameter will diverge to infinity; that is, flat lamellar sheets are the predicted self-assembly product. DC(8,9)PC *R*-, *S*- enantiomer-mixing experiments have failed to show this; indeed the racemate produces left- and right-handed tubules of unchanged diameter.[28] This outcome has been explained by positing a spontaneous DC(8,9)PC enantiomer separation that occurs in the course of tubule formation; in this way, tubule handedness remains traceable down to the dimensions of chiral molecular packing. This enantiomeric separation is well precedented; indeed Pasteur's resolution of D- and L-tartaric acids through the painstaking microscopic examination and subsequent separation of crystal habit is the basis of modern experimental stereochemistry.[29]

The presence of two crystal habits (left- and right-handed helices) in our enantiopure phosphonate preparations, however, is inconsistent with a chiral-packing mechanism. While the evolution of left- and right-handed helices in mixed-enantiomer DC(8,9)PC systems has been reasonably interpreted in terms of chiral-packing theory, the experimental outcome does not exclude the possibility that a chiral symmetry-breaking mechanism is operative. Specifically, it is possible that the intended zero net-chirality state of the DC(8,9)PC enantiomer-mixing experiment was in fact attained and that the subsequent formation of left- and right-handed helices is reflective of the random nature of the chiral symmetry-breaking mechanism. This interpretation does not link tubule diameter to enantiomeric excess, which is consistent with the enantiomer-mixing outcome, and it also obviates the postulated enantiomeric separation. Nevertheless, the enantiomer separation/chiral-packing models remain a valid possibility.

The profound morphological differences between DC(8,9)PC and tubules made from either phosphonate, as well as the smaller, but distinct changes between "C3" and "C4" phosphonate tubules, are our first steps in delineating the dependence of tubule formation upon the so-called "backbone" of the tubule-forming molecule. The dramatic effects evoked by minor modifications about the chiral center within this backbone

(25) Seifert, U.; Shillcock, J.; Nelson, P. *Phys. Rev. Lett.* **1996**, *77*, 5237−5240.
(26) Dierker, S. B.; Pindak, R.; Meyer, R. B. *Phys. Rev. Lett.* **1986**, *56*, 1819−1822.
(27) Kamien, R. D.; Selinger, J. V. *J. Phys.: Condens. Matter* **2001**, *13*, R1−R22.
(28) Spector, M. S.; Selinger, J. V.; Schnur, J. M. *J. Am. Chem. Soc.* **1997**, *119*, 8533−8539.
(29) Eliel, E. L.; Wilen, S. H.; Mander, L. N. *Stereochemistry of Organic Compounds*; John Wiley & Sons: New York, 1994.

suggest that additional bond length and angle modifications may produce tubules of new, technologically useful and theoretically interesting dimensions. That no significant loss of tubule-forming capacity has occurred thus far supplies additional motivation to continue the synthetic strategy we have undertaken. While the results of this report are in general supportive of chiral symmetry-breaking models, the striking uniformity of handedness found in enantiopure DC(8,9)PC preparations demands that molecular chirality, absent in chiral symmetry-breaking models, be included in tubule formation theory.

**Acknowledgment.** B.N.T. was supported by NSF CAREER Grant CHE-9734266. Acknowledgment is made by B.N.T. to the donors of the Petroleum Research Fund, administered by the American Chemical Society, for partial support of this research. J.E.K. was supported in part by a Research and Training Program award of the Exxon Education Foundation. C.L.C. was supported by a University of Wyoming Grant-In-Aid. We thank Professor David L. Johnson of the University of Oklahoma Health Sciences Center Department of Occupational & Environmental Health for discussions regarding fibrous aerosols. High-resolution mass spectra were obtained by the Washington University Resource for Biomedical and Bioorganic Mass Spectrometry at Washington University, St. Louis, Missouri. Portions of this work were executed at Beamline X20A of the National Synchrotron Light Source at Brookhaven National Laboratory, administered by the United States Department of Energy.

JA012137A